Available online at www.sciencedirect.com
SCIENCE DIRECT
Journal of the European Ceramic Society 26 (2006) 1743–1752
www.elsevier.com/locate/jeurceramsoc

Verification of the stresses developed in silicon nitride by repeated thermal shocks

Ernest Gondar *, Tomas Hlava, Miroslav Rosko

Faculty of Mechanical Engineering, Pionierska 15, 831 02 Bratislava, Slovak Republic

Received 30 October 2004; received in revised form 10 March 2005; accepted 26 March 2005
Available online 10 May 2005

Abstract

A new testing method was used to test the resistance of silicon nitride to repeated thermal shocks. Specimens with cracks initiated by Vicker's indentor were cyclically heated to 1100 °C and cooled to 500 °C. Temperature and stress progress was computed in two points. One point was located on the surface of the specimen and the other one in a region that is most dangerous for crack growth. The temperature progress of the surface point was verified using a thermocouple. First thermal shock caused the highest temperature peak and amplitude. The temperature stabilised after different number of cycles in the two analyzed points. Stress oscilation had a different character. We defined an increasing, a stabilised and a decreasing stage. Calculated critical stress, needed for unstable crack growth (132.2 MPa) was assigned to the 13th stress peak. During practical experiments, unstable crack growth occured after the 4th cycle (114.9 MPa). The difference between this value and the value of calculated critical stress was 15%.

Keywords: Thermal shock resistance; Testing; Si_3N_4

1. Introduction

The important position of silicon nitride in industry is given by its properties, especially its high-temperature strength and resistance to thermal shocks. Several methods have been invented to test this resistance. Indentation-quenching method is the one most widely used. A specimen with initiated cracks is heated to a certain temperature in an oven and then rapidly quenched, usually by falling into water.[1–3] This way the specimen is subjected to a thermal shock. Several modifications of this method have been introduced, for example a modification that allows a more rapid thermal shock by avoiding phase changes of the quenching medium.[4] The disadvantage of the indentation-quenching method is a significant time consumption when dealing with repeated thermal shocks. This disadvantage can be removed by using high-energy fields, such as laser or tungsten lamp heating.[5–7] These methods allow to determine boundary conditions for a simulation of temperature and stress in the material by analytical approximation.[8] The aim of our research is simulation and verification of the temperature and stress fields in silicon nitride generated during repeated thermal shocks.

2. Experimental

In the Department of Materials and Technologies of the Faculty of Mechanical Engineering of Slovak Technical University, a new testing method has been developed[9] and optimised[10] to test the resistance of technical ceramics to repeated thermal shocks. The principle of this method is shown in Fig. 1. Specimens of circular cross-section (1) are being used in this test, with cracks (3) formerly initiated by Vicker's indentor. The specimen is placed with its damaged side (2) facing downwards and this side is constantly (without interruptions) cooled by water. Its opposite side is cyclically

* Corresponding author. Tel.: +421 2 444 55087; fax: +421 2 444 55091.
E-mail address: ernest.gondar@stuba.sk (E. Gondar).

0955-2219/$ – see front matter © 2005 Elsevier Ltd. All rights reserved.
doi:10.1016/j.jeurceramsoc.2005.03.255

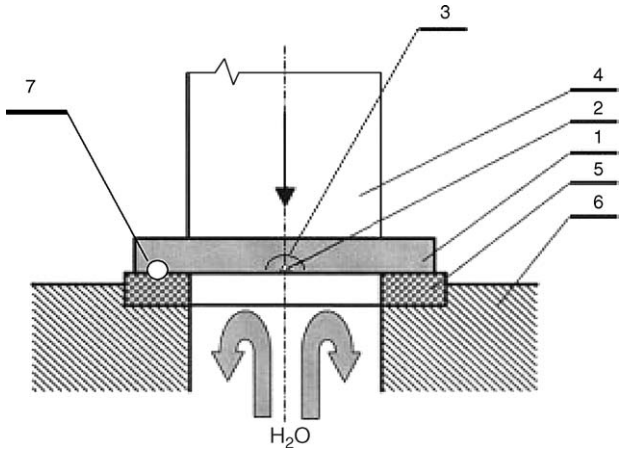

Fig. 1. Principle of the new method of testing the resistance of silicon nitride to repeated thermal shocks. 1, Specimen; 2, indent; 3, crack; 4, punch; 5, sealing; 6, support; 7, position of thermocouple.

heated using a punch (4). The punch is heated by an induction coil and is loaded by a 6 kg weight. This weight prevents the cooling water from leaking from under the sealing. The diamater of the punch is equal to the hole diamater of the sealing. This way, the only mechanical loading of the specimen is shear acting under the perimeter of the punch. Mechanical loading acting on the indent and the cracks is negligible. The type of mechanical loading can be changed by modifying the punch diameter. The principle of the new testing method is at present applying for a patent.[11] The method allows testing of specimens using a large range of parameters, such as heating and cooling time and temperature (which defines the thermal shock), diameter of the punch (modifying the amount of heat entering the specimen, as well as the type of mechanical loading) and the dimensions (diameter and thickness) of the specimen. The main advantage of the method is low time consumption and the possibility to define boundary conditions for computer simulation of temperature and stress fields. Hence, it can be used to verify the simulation by practical experiments.

The specimens were prepared by cold pressing and then hot pressing in nitrogen (N_2) atmosphere. Activating agents of silicon nitride were Al_2O_3 and Y_2O_3 with mass ratio:

$$85.36\,\text{wt.\%}\ Si_3N_4 + 10.34\,\text{wt.\%}\ Y_2O_3 + 4.30\,\text{wt.\%}\ Al_2O_3$$

This mass ratio corresponds to 10% YAG. The hot pressing of the experimental material took place on a laboratory hot press with a special construction of heating body.[12] The prepared specimens were of 2 mm thickness with 8 mm diameter. After metallographic preparation of the specimens, cracks were initiated in them using Vicker's indentor with parameters: loading force, $F = 294.3$ N; loading time, $t = 15$ s; temperature, $T = 20\,^{\circ}\text{C}$

Fracture toughness of the specimens was determined from the dimensions of indents and of the cracks.

The depth profile of cracks was determined by horizontal serial sectioning of the material, as well as from the observation of fracture areas.[13] A similar method was described also in,[14] where serial sectioning took place in vertical direction (perpendicular to the damaged surface).

The specimens were repeatedly heated to 1100 °C and cooled to 500 °C. The duration of the heating and cooling cycle was 16 s and 5 s, respectively (Fig. 2). These temperatures were measured using a thermocouple located between the punch and the specimen, as well as using a pyrometer.

To determine the stresses and temperatures in the material, finite element method was utilised, using software ANSYS. One quarter of the specimen was modeled according to our knowledge of the depth profile of the crack. Zero displacement of relevant areas due to symmetry of

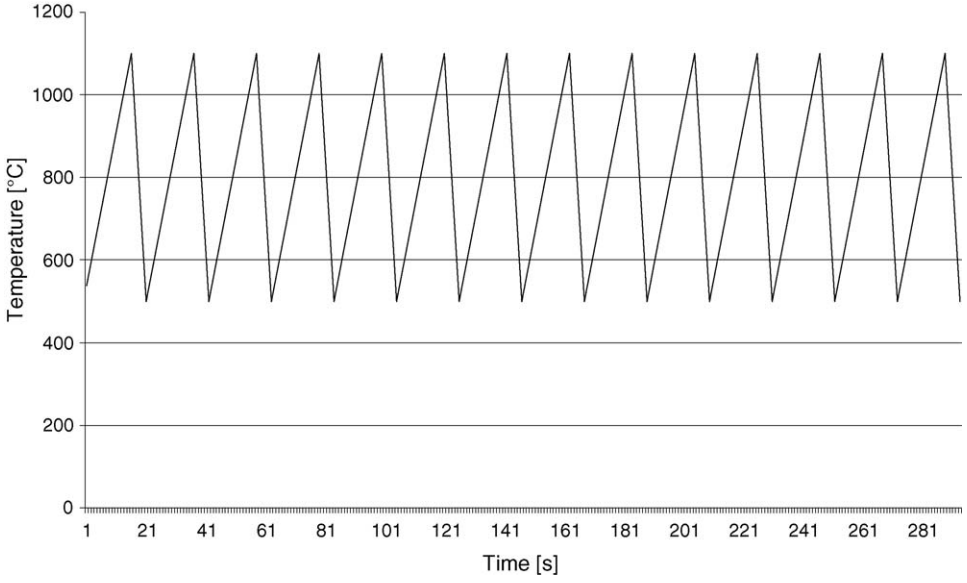

Fig. 2. Temperature progress on the heated side of the specimen.

Table 1
Material properties entered into the simulation

Material property	Value	Units
Thermal conductivity	24.0	$W\,m^{-1}\,K^{-1}$
Specific heat capacity	705.0	$J\,kg^{-1}\,K^{-1}$
Density	3200.0	$kg\,m^{-3}$
Young's modulus of elasticity	315.0×10^9	Pa
Poisson's ratio	0.27	–
Thermal expansion coefficient	3.2×10^{-6}	K^{-1}
Surface heat transfer (cooled side of the specimen)	50,000	$W\,m^{-2}\,K^{-1}$
Surface heat transfer (rest of the specimen)	0.5	$W\,m^{-2}\,K^{-1}$

this quarter was also defined. The chosen element type was SOLID70, a thermal solid with 3D thermal conduction capability, which is applicable to a 3D transient thermal analysis. Material properties entered into the simulation are shown in Table 1.

The computed values of temperature were verified by measuring real temperature using a thermocouple (Fig. 1, point 7). Stresses from the computer simulation were also verified. First, critical stress needed for unstable crack growth was calculated from the fracture toughness of the most dangerous area for crack propagation. This area was located on the depth profile of initiated cracks. A series of experiments was performed to determine the cycles, after which unstable crack growth occurs. From the simulation output we obtained the value of stress during this particular cycle. Finally, the calculated critical stress and the stress obtained from the computer simulation was compared.

Several generalized assumptions were taken into account during the solution of the problem. These assumptions are based on the results which have been published so far and they were utilized by determination of the critical stress, critical dimension of the crack and the physical properties of the testing material.

3. Results and discussion

Sketch of the depth profile is shown in Fig. 3. Point 1 represents the end of the crack on the surface, point 2 lies on the edge of the crack under the deformed zone, which was created under the indent during indentation.

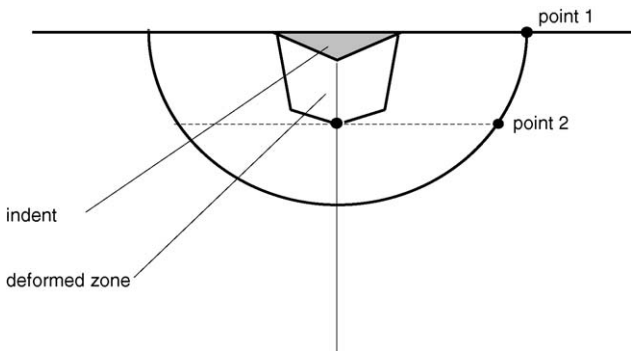

Fig. 3. Depth profile of the crack, definition of point 1 and point 2.

The depth and shape of this area was different from the ones stated in literature.[15,16] The shape is angular, block-like with a sharp pyramidal tip. Cracks, initiated with Vicker's indentor, are circumventing the deformed zone. Its depth, obtained from our experiments, as well as from the fracture areas ranges from 120 μm to 140 μm. For calculation of the depth, following formula is used:[17]

$$h \approx \left(\frac{p}{H}\right)^{1/2}\left(\frac{E}{H}\right)^{2/5} \quad (1)$$

where: p is indentation loading force [N]; H is Vicker's hardness [MPa]; E is Young's modulus of elasticity [MPa]

Substituing $E = 310$ GPa into this formula will give us a depth of more than 400 μm. Hence, in our case this formula cannot be used for calculation of the depth of the deformed zone.

The fracture toughness of the specimen was calculated from the length of the cracks using the formula:

$$K_{IC} = 0.129\left(\frac{c}{r}\right)^{-3/2}\left(\frac{E}{H_v}\right)^{2/5}\frac{H_v r^{1/2}}{k}$$

where $2c$ is the total surface crack length [m]; $2r$ is the length of the indent's diagonal [m]; E is Young's modulus of elasticity [MPa]; H_v is Vicker's hardness [MPa]; k is dimensionless constraint factor, $k = 3$.

Calculated value of fracture toughness was 4.8 MPa $m^{1/2}$.

The most dangerous region for crack growth was determined from a detailed analysis of the crack's depth profile.[18] The half-penny shape of the crack suggests using a formula $\sigma = K_{IC}/0.72\sqrt{\pi c}$[19] (where K_{IC} is fracture toughness and c is the crack depth), but deepening of the crack is not a dominant direction of its growth. The dominant direction of crack growth is sideways, in subsurface layers.[20] Another possibility would be to approximate a formula for a half-annular crack. However, this would be in contrast to the shape of the deformed zone, which is in the form of a truncated pyramid, with a sharp pyramidal tip.[18] Angular shape of the deformed zone does not copy the round shape of the crack profile. Although the depth profile does not correspond to a central surface crack, the formula $\sigma = K_{IC}/\sqrt{\pi c}$ will be used for calculation of the critical stress, because of the expected direction of crack growth. On the basis of these facts, the region under the deformed zone (dashed line in Fig. 3), with crack length of 420 μm, has been considered as the most dangerous for crack growth. This region allows growth of the crack sideways, in subsurface layers, which is a preferred direction.[20]

Minor cracks,[18] which are shorter but more numerous than the major indentation cracks, were not taken into account when determining the most dangerous region for the crack growth. The growth of these minor cracks during thermal shocks has not been experimentally proved.

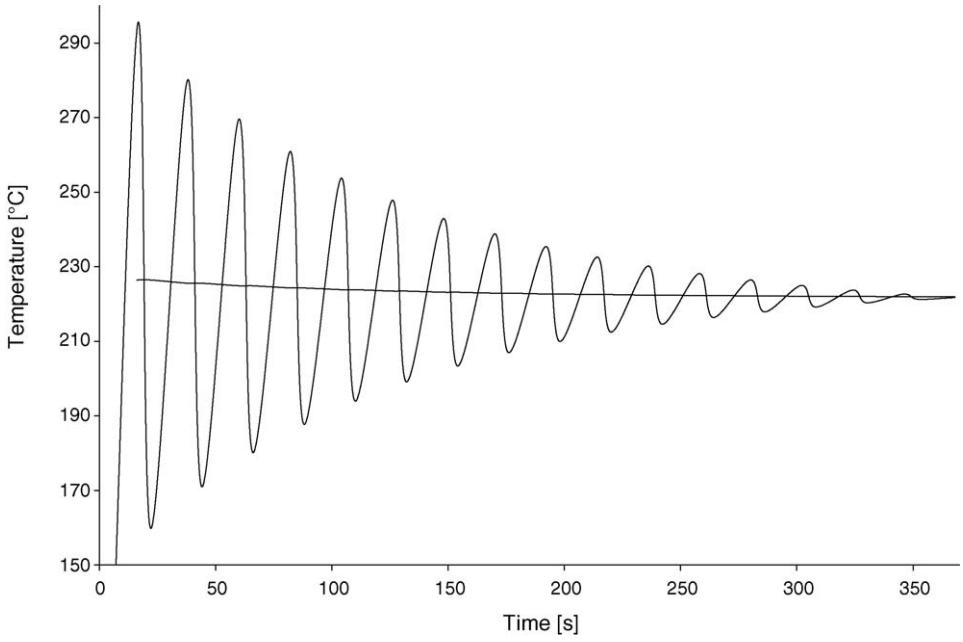

Fig. 4. Temperature progress between the specimen and the sealing—simulation output.

Critical stress, needed for crack growth was calculated from the formula:

$$\sigma = \frac{K_{IC}}{\sqrt{\pi c}} \text{ [MPa]} \quad (2)$$

where K_{IC} is fracture toughness [MPa m$^{1/2}$]; c is the crack length [m]

The calculated critical stress for point 2 was 132.2 MPa. Critical stress, calculated for point 1 (Fig. 3) was 221.12 MPa.

A direct control of temperature progess in point 1 and 2 is practically impossible, hence the temperature was measured between the sealing and the specimen (Fig. 1, point 7) using a thermocouple. We also made a simulation of temperature progress in this point. The simulation output can be seen in Fig. 4. First thermal shock caused the highest amplitude (133 °C). The temperature amplitude was decreasing in time and after approximately 16 cycles it stabilised at a value of only 1 °C. The temperature peaks stabilised from 293 °C (1st cycle) to 222 °C (16th cycle). The mean temperature changed

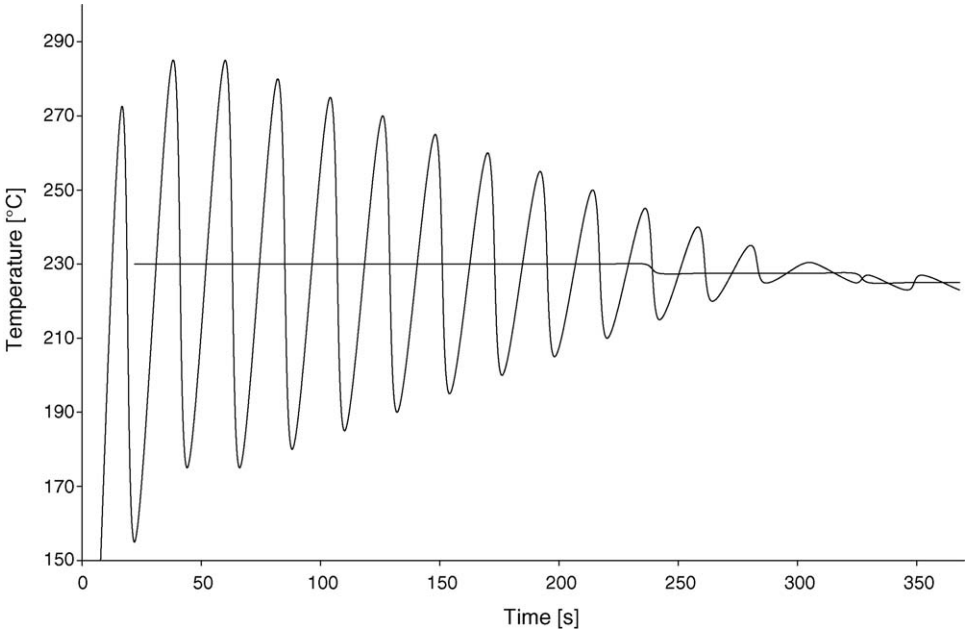

Fig. 5. Temperature progress between the specimen and the sealing—measured values.

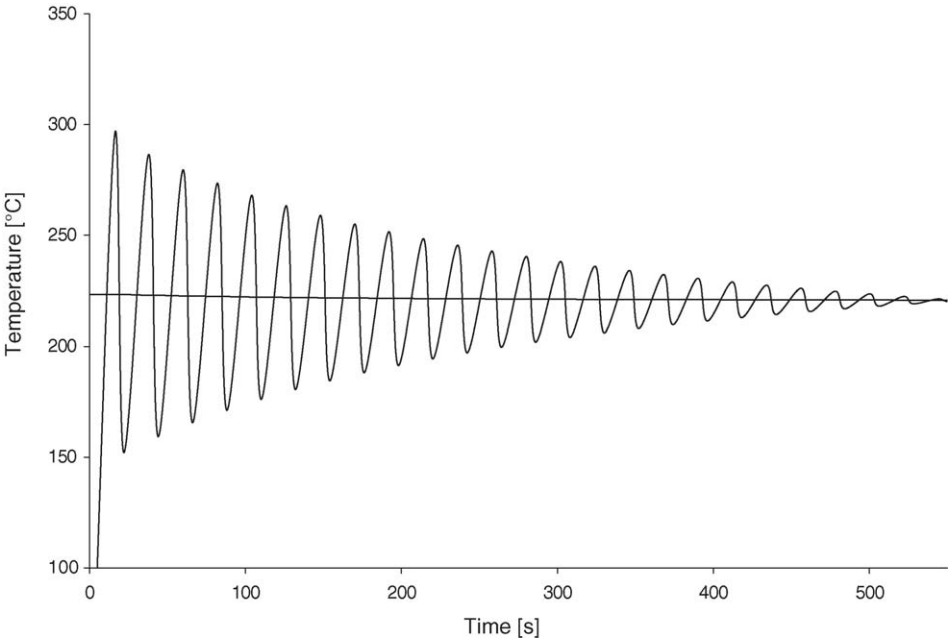

Fig. 6. Temperature progress in point 2, 25 cycles.

smoothly from 226 °C at the beginning to 221.5 °C in the 16th cycle. The temperature progress thus represents damping of the initial highest amplitude to the mean value.

The measured values of temperature under the sealing are shown in Fig. 5. It can be seen, that the temperature progress is the same, as is the number of cycles needed for stabilisation. Both amplitudes and peaks of the measured temperatures are higher than the ones of the computed temperatures—the only exception is the first cycle. The mean temperature remains constant (230 °C) during the first 10 cycles. In the 11th cycle, it drops to 227.5 °C and in the 15th cycle there is another drop—to 225 °C. Despite the differencies stated above, the computed and measured temperature progress are in good accordance and the simulation can be considered verified.

Temperature progress in the critical point 2 (Fig. 3) from the simulation output for 25 cycles is shown in Fig. 6. The character of oscillation was the same as in point 7 discussed above. Highest amplitude (142.3 °C) was again caused by the first thermal shock. The temperature amplitude stabilised at a value of 1 °C after 24 cycles. The mean temperature decreased from 223.3 °C to 220.5 °C. Maximal temperature during the first cycle was 294.4 °C.

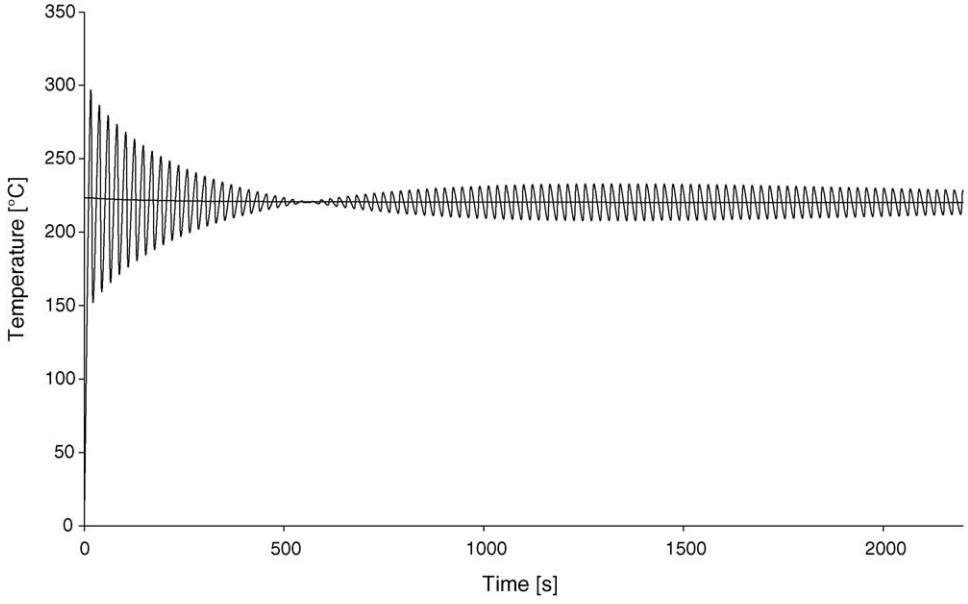

Fig. 7. Temperature progress in point 2, 100 cycles.

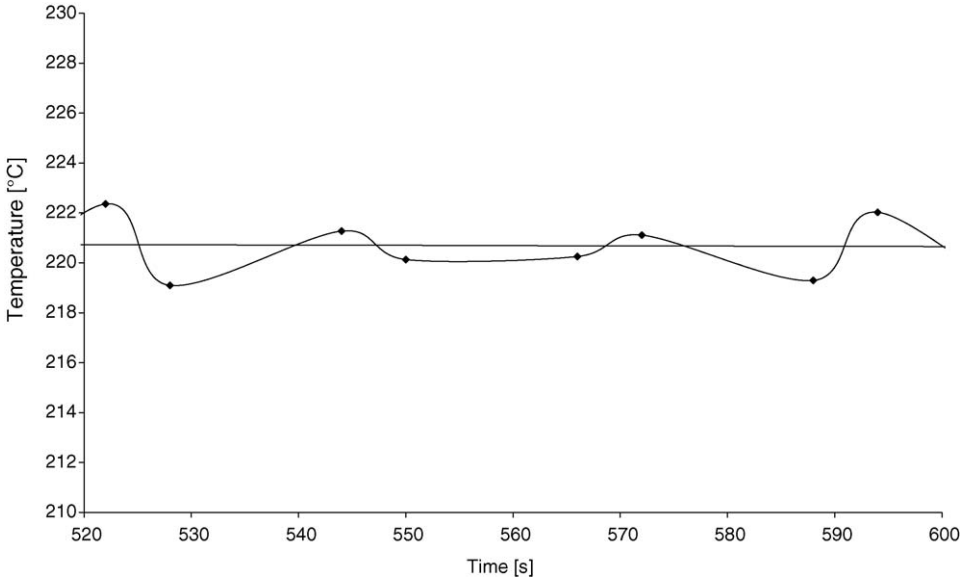

Fig. 8. Detail of temperature stabilisation in point 2.

The stabilisation of temperature is not final. Fig. 7 shows temperature progress in point 2 during 100 cycles. After stabilisation in the 24th cycle, another stage of oscillation starts with an increasing amplitude, which reaches its maximal temperature (232.86 °C) after the 60th cycle. Afterwards, the oscillation stabilises again slowly. The character of the oscillation is different in the second stage when compared to the first one. Fig. 8 shows a detail of the stabilisation between first and second stage. It can be seen, that during stabilisation the heating cycle (16 s, from 550th to 566th second) does not cause a significant rise of temperature (only 0.118 °C). The temperature then rises over the mean value during the cooling cycle (6 s). The oscillation progress is henceforward mirrored in comparison with the first stage. An even longer temperature progress in point 2 (200 cycles) is shown in Fig. 9. It is clear that the temperature oscillation stabilises in several stages, each of them having a lower amplitude. There is another mirroring between the second and third stage, hence the character of oscillation in the third stage is analogical to the one in first stage.

The stress progress was analyzed in point 1 on the surface and in the critical point 2 (Fig. 3). Stress progress in point 1 is shown in Fig. 10. The amplitude increased from a starting value of 31.2 MPa to 141.1 MPa in the

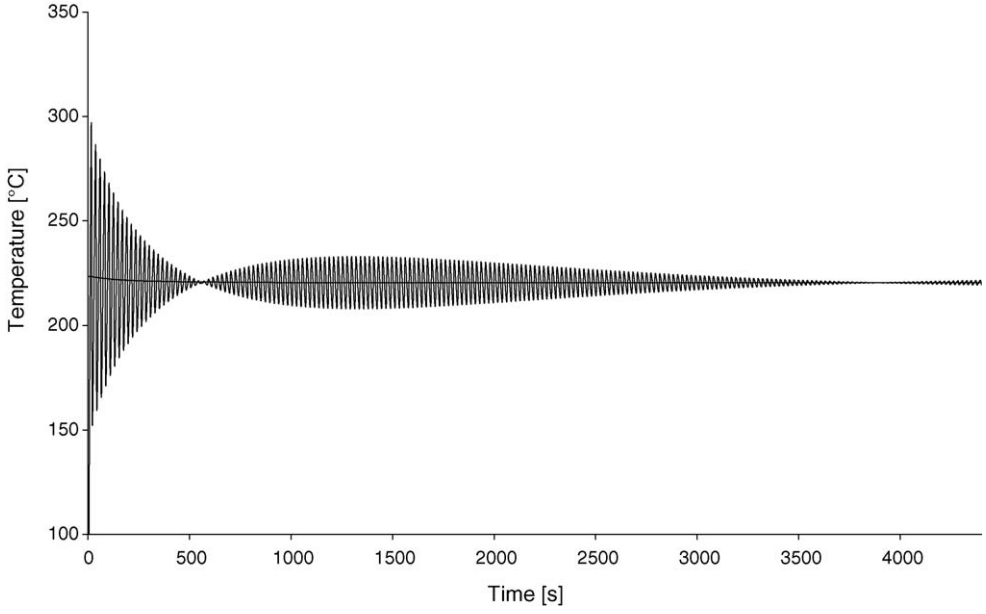

Fig. 9. Temperature progress in point 2, 200 cycles.

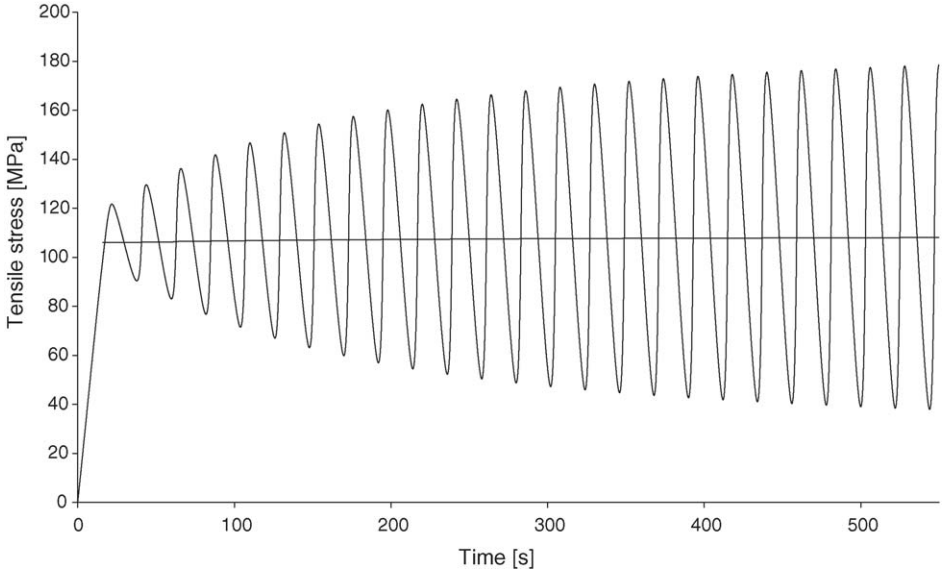

Fig. 10. Stress progress in point 1, 25 cycles.

25th cycle. Maximal stress increased from 121.7 MPa (for the first thermal shock) to 178.6 MPa (25th shock). The stress was considered stabilised, if the difference between the previous and next cycle's peak was not greater than 0.5%. In our case, this state was reached after 20 thermal shocks. The difference further decreases and between the 24th and 25th peak it represents only 0.34%. Hence, the first 20 cycles represent a so called increasing stage and the following cycles represent a stabilised stage. In the increasing stage, the highest difference (between the first and second stress peak) represents 6.5%. The mean stress changed from 106.1 MPa during the first cycle to 108 MPa during the 25th one. This change is negligible, as it represents only approximately 1.8%. It is important to note that the critical stress, calculated for point 1 (221.12 MPa) was not reached even in the last cycle. That means, that none of the 25 thermal shocks should cause crack growth.

Fig. 11 shows the stress progress during 25 cycles in the critical point 2. Character of oscillation is again the same as in point 1. The stabilised stage was reached after 16 cycles, the difference between the 24th and 25th peak represents only 0.15%. The maximal stresses in point 2 are on average 27% lower than the ones in point 1. They increased from 99.2 MPa to 137.9 MPa. Since the calculated critical stress, necessary for crack growth (132.2 MPa) is within this range, the simulation could be experimentally verified. The value of maximal stress during the 13th cycle is 132.7 MPa, hence

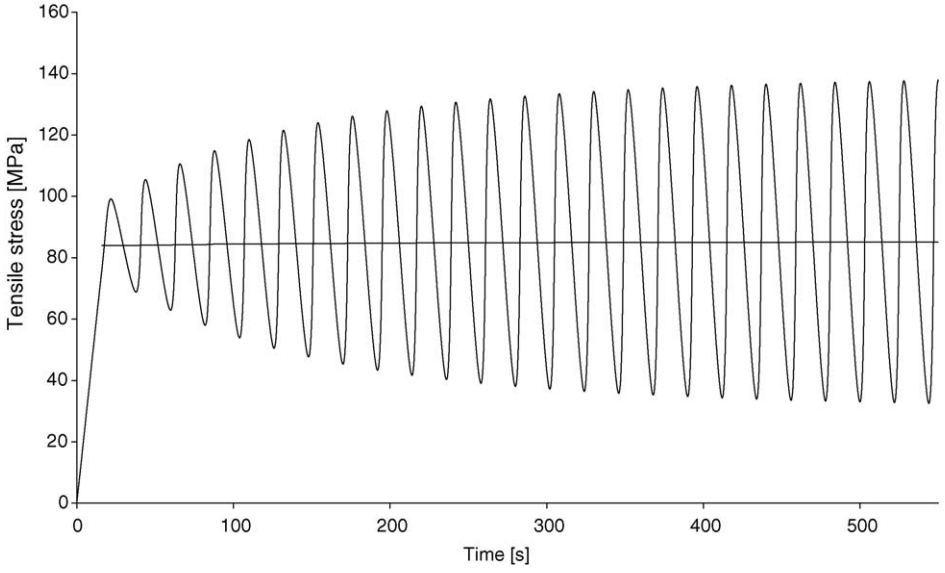

Fig. 11. Stress progress in point 2, 25 cycles.

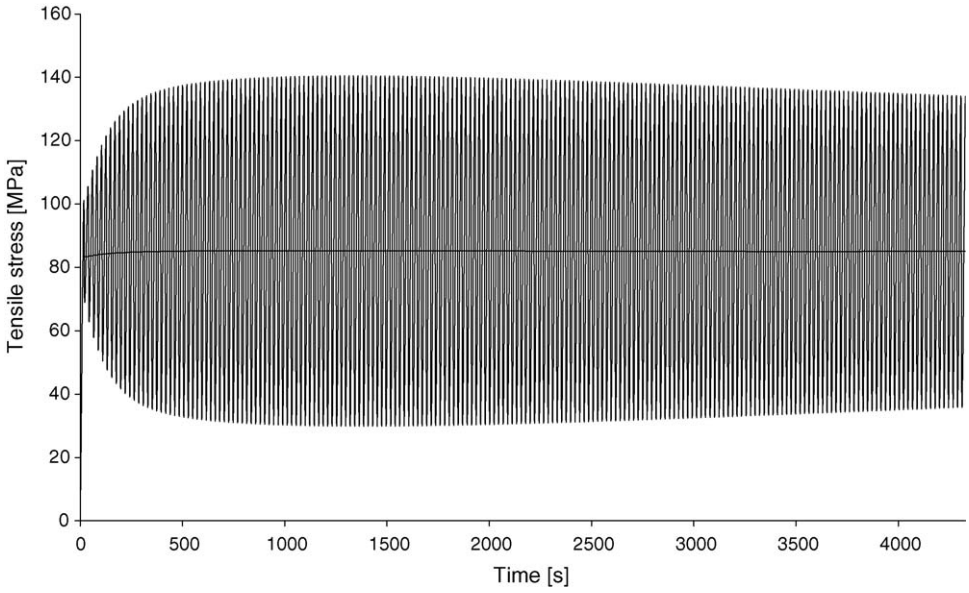

Fig. 12. Stress progress in point 2, 200 cycles.

the critical stress could be assigned to this peak quite exactly (with difference of only 0.38%).

The relation between the temperature and stress is, that the first temperature stabilisation practically corresponds to the stabilisation of stress at its maximal value. A question may arise, how can temperature, stabilised on a constant value, lead to any stress oscillation. The damping of temperature oscillation is similar to damping of a spring system. Fig. 12 shows the stress progress in point 2 for 200 cycles. After increasing and stabilising stage follows a decreasing stage. The main reason for this behaviour and for the stepwise stabilisation of temperature follows from the conditions of the test. We assume that a simple stabilisation is hindered by small dimensions of the specimen and by the amount of heat entering the specimen. The thickness of the specimen is only 2 mm. This assumption was confirmed by performing a simulation with specimen thickness of 20 mm. The resulting temperature progress in point 2 is shown in Fig. 13. It can be seen, that the first stabilisation occurs after the 6th cycle and the second stabilisation (after 16th) cycle is final. Maximal amplitude during the first oscillation is 0.89 °C, during the second oscillation it is only 0.07 °C. Low amplitudes can be seen also in the stress progress in this point (Fig. 14). Under these conditions, temperature and stress oscillation are of similar character. Maximal stress amplitude is only 1.12 MPa (3rd cycle). The oscillation smoothly stabilises, the amplitude af-

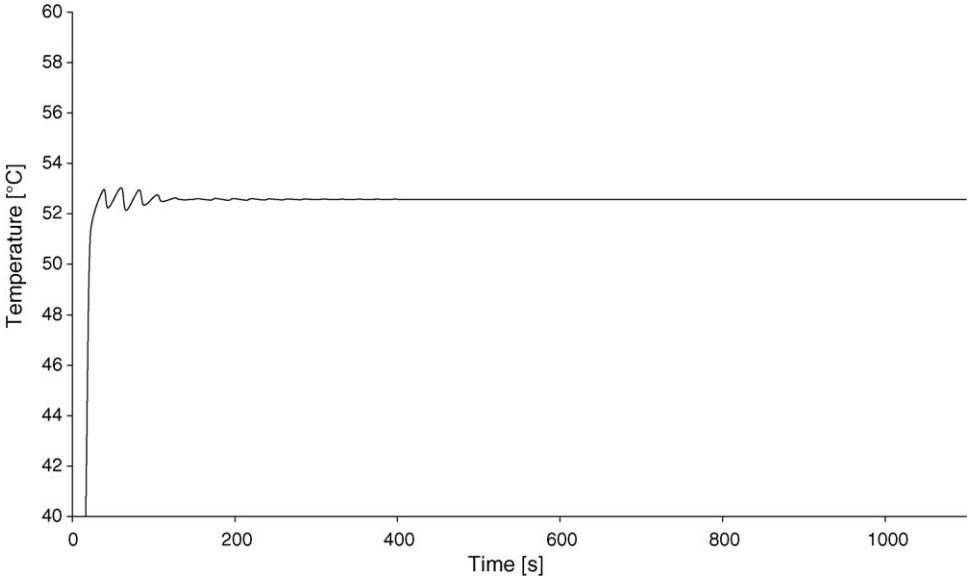

Fig. 13. Temperature progress in point 2, specimen thickness 20 mm, 50 cycles.

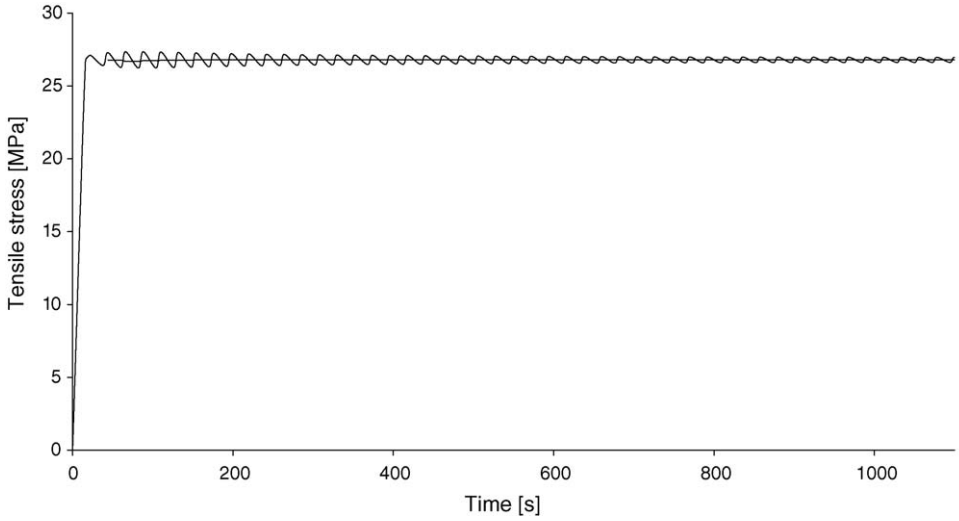

Fig. 14. Stress progress in point 2, specimen thickness 20 mm, 50 cycles.

ter 30 cycles is 0.5 MPa and after 50 cycles it is negligible (0.29 MPa).

An analysis of temperature and stress fields of the whole specimen, however, would be too complicated and would exceed the scope of this contribution.

During practical experiment, the specimen was first subjected to 20 thermal shocks, because the stress in point 2 after 20 cycles is almost stabilised at its maximal value (Fig. 11). The difference between the 20th and 21st cycle is only 0.3%. After testing it could be seen, that unstable crack growth occured. We decreased the number of cycles gradually (using a new specimen for each experiment) to determine the lowest number of cycles, at which crack growth occurs. The results can be seen in Table 2. From these experiments follows, that the lowest number of cycles needed for crack growth is 4 (with 80% reliability). The real stress needed for crack growth thus lies between 110.6 MPa (3rd cycle, Fig. 11) and 114.9 MPa (4th cycle). The difference between these two peaks is 3.9% and it can be considered as the relative error of the assignment. The difference between the calculated critical stress (132.2 MPa) and the stress obtained from computer simulation (4th cycle) is 17.3 MPa, i.e. 15%. This result is very promising and opens wide possibilities for further experiments and refinement of the simulation.

Table 2
Results of practical experiments

Specimen no.	Cycles applied	Result
1	20	Crack growth
2	15	Crack growth
3	10	Crack growth
4	5	Crack growth
5	5	Crack growth
6	3	Crack length unchanged
7	4	Crack growth
8	5	Crack growth
9	4	Crack growth
10	3	Crack length unchanged
11	3	Crack length unchanged
12	3	Crack length unchanged
13	3	Crack length unchanged
14	4	Crack growth
15	4	Crack length unchanged
16	4	Crack growth

4. Conclusion

A new testing method was introduced to test the resistance of technical ceramics to repeated thermal shocks. Specimens of silicon nitride were cyclically heated to 1100 °C and cooled to 500 °C. Duration of one cycle was 22 s.

Cracks were formerly initiated in the specimens using Vicker's indentor. The depth profile of these cracks and the shape of deformed zone under the indent was determined by horizontal serial sectioning and from the study of fracture areas. The results do not correspond to the ones published earlier.

The most dangerous area for crack growth was located on the depth profile of the crack under the deformed zone. Calculated critical stress for this region is 132.2 MPa; critical stress for crack edge on the surface is 221.12 MPa. Several generalized assumptions were utilized by determination of the critical crack length and critical stress.

Temperature progress on the surface of the specimen was verified experimentally. Character of the temperature progress was the same also for the critical region under the deformed zone. First thermal shock caused the highest amplitude and maximal temperature. After 16 cycles, the temperature on the surface stabilised at the mean value of 221.5 °C. The temperature under the deformed zone stabilised after 24 cycles at 220.5 °C. The temperature stabilisation was stepwise, analogical to a spring system.

The stress progress was different. First thermal shock caused the lowest stress peak and amplitude. During the next cycles, both amplitude and maximal stresses were increasing and after a certain number of thermal shocks they stabilised. Thus we defined an increasing stage, a stabilised stage and a decreasing stage. A relation between temperature and stress progress was shown.

On the surface, the stabilised stage was reached after 20 cycles. Maximal stress increased from 121.7 MPa (1st cycle) to 178.6 MPa (25th cycle). The critical stress needed for crack growth (221.12 MPa) was not reached for this point. In the critical point under the deformed zone, the maximal stress increased from 99.2 MPa (1st cycle) to 137.9 MPa (25th cycle). The stabilised stage was reached after 16 cycles. Critical stress for this point (132.2 MPa) was assigned to the 13th peak, with difference of only 0.38%.

During practical experiments, the crack growth occured after the 4th cycle. Computed value of stress during this cycle was 114.9 MPa. The difference between this value and the value of calculated critical stress (132.2 MPa) was 15%.

References

1. Andersson, T. and Rowcliffe, D. J., Indentation thermal shock test for ceramics. *J. Am. Ceram. Soc.*, 1996, **79**, 1509–1514.
2. Glandus, J.C. and Tranchand, V. Thermal shock by water quench: numerical simulation, thermal shock and thermal fatigue behaviour of advanced ceramics. *Nato ASI Series, Series E: Applied Sciences, Vol. 241*, 1993, pp. 307–316.
3. Koh, Y. H., Kim, H. W., Kim, H. E. and Halloran, J., Thermal shock resistance of fibrous monolithic Si_3N_4/BN ceramics. *J. Eur. Ceram. Soc.*, 2004, **24**, 2339–2347.
4. Absi, J. and Glandus, J. C., Improved method for severe thermal shock testing of ceramics by water quenching. *J. Eur. Ceram. Soc.*, 2003, **24**, 2835–2838.
5. Vedula, V. R., Green, D. J., Hellmann, J. R. and Segall, A. E., Test methodology for thermal shock characterization of ceramics. *J. Mater. Sci.*, 1998, **33**, 5427–5432.
6. Schaus, M. and Pohl, M., Nd-YAG-LASER simulated thermal shock and thermal fatigue behaviour. *Metallurgy*, 1998, **5**, 464.
7. Akiyama, S. and Amada, S., New method to evaluate the thermal shock resistance of ceramics by laser pulse irradiation. *Fusion Technol.*, 1993, **23**, 426–434.
8. Collin, M. and Rowcliffe, D., Analysis and prediction of thermal shock in brittle materials. *Acta Mater.*, 2000, **48**, 1655–1665.
9. Gondar, E., Pulc, V. and Krizanska, M., Testing the resistance of technical ceramics to thermal loading. In *Technologia 95*, 1995, p. 34.
10. Gondar, E., The testing method of resistance of silicon nitride based technical ceramics to thermal loading. In *Conferment Project*, 1998.
11. Pulc, V., Gondar, E. and Svec, P., *Testing Method of the Resistance of Technical Ceramics to Thermal Fatigue*, Patent Pending 518-2001.
12. Pulc, V., Gondar, E. and Svec, P., Equipment for hot pressing of powders. In *International Conference*, 1992, p. 97.
13. Rosko, M., Study of default defects in silicon nitride, In *Proceedings Strojne inzinierstvo 2004*.
14. Lube, T., Indentation crack profiles in silicon nitride. *J. Eur. Ceram. Soc.*, 2001, **21**, 211–218.
15. Reece, M. and Guiu, F., Repeated indentation method for studying cyclic fatigue in ceramics. *J. Am. Ceram. Soc.*, 1990, **73**, 1004–1013.
16. Horvathova, J., Olejnickova, L., Jonsta, Z. and Mazanec, K., Fractographic analysis of conditions leading to the crack formation during the indentation loading. *Fractography 2003*. Institute of Material Research SAV Kosice, 2003, p. 94.
17. Evans, A. G. and Wilshaw, T. R., Quasistatic particle damage in brittle solids. *Acta Metall.*, 1976, **24**, 939–956.
18. Gondar, E., Rosko, M. and Zemankova, M., Study of depth profile of indentation cracks in silicon nitride. *Metal. Mater.*, 2005, **43**, 124–133.
19. Broek, J. D., *Elementary Engineering Fracture Mechanics*. Noordhoff International Publishing, Leyden, 1974.
20. Collin, M. and Rowcliffe, D., The morphology of thermal cracks in brittle materials. *J. Eur. Ceram. Soc.*, 2002, **22**, 435–445.